# Ligand Charge Separation to Build Highly Stable Quasi-Isomer of MOF-74-Zn

Huajun Yang,<sup>a</sup> Fang Peng,<sup>a</sup> Candy Dang,<sup>a</sup> Yong Wang,<sup>b</sup> Dandan Hu,<sup>b</sup> Xiang Zhao,<sup>b</sup> Pingyun Feng\*,<sup>b</sup> and Xianhui Bu\*,<sup>a</sup>

ABSTRACT: Built from an unusual high-charge-density ligand 2,5-dioxido-1,4-benzenedicarboxylate (dobdc<sup>4-</sup>), MOF-74M (M<sub>2</sub>dobdc) have unsurpassed gas uptake and separation properties. It is thus intriguing to mimic or replicate such ligand properties in other chemical systems. Here, we show a ligand charge separation (LCS) model that could offer one pathway towards this goal. Two new materials (CPM-74 and -75, corresponding to MOF-74 and IRMOF-74-II, respectively) are presented here to illustrate this concept and its feasibility. Specifically, dobdc<sup>4-</sup> ligand in MOF-74 can be conceptually broken down into OH- and obdc<sup>3</sup>- (H<sub>3</sub>obdc = 2-hydroxyterephthalic acid), which leads to CPM-74, Zn<sub>2</sub>(OH)(obdc), that is nearly isomeric with MOF-74-Zn. Different from MOF-74, CPM-74 is made from homo-helical rod packing. Moreover, CPM-74 has high hydrothermal and thermal stability uncommon for Zn-MOFs. It contains open Zn sites on 4coordinated Zn<sup>2+</sup> and its isosteric heat of adsorption for CO<sub>2</sub> is 22% higher than that of MOF-74-Zn at low pressures.

The density and bonding environment of metal sites in metalorganic frameworks (MOFs) are important considerations in the synthetic design of crystalline porous materials (CPM) because they play key roles in porosity, stability, and functionality. Recent advances in MOFs, particularly, in the aspect of ligand design, have led to an unprecedented success in creating large ligands and MOFs such as meso-MOFs or IRMOFs with high porosity, low density of metal sites, and novel applications.<sup>1-7</sup> In comparison, synthetic efforts to make MOFs with a high density of metal sites are less methodical. Such MOFs can be advantageous for many applications.8-20 ENREF 7 ENREF 7 For MOFs with a high density of metal sites may not only enhance gas adsorption capacity and selectivity under ambient conditions, 21-23 but also contribute to high stability and a high density of active sites. 10,24-34 ENREF 16

A simple charge-balance analysis indicates that an important contributing factor to the high-density metal sites is the high negative charge density of the ligand. For  $M^{2+}$ -based MOFs,

MOF-74 (or CPO-27),<sup>35-37</sup> its isomers (M<sub>2</sub>m-dobdc,<sup>38,39</sup> UTSA-74<sup>40</sup>), and its thio-analog<sup>41,42</sup> (H<sub>4</sub>m-dobdc = 4,6-dihydroxy-1,3-benzenedicarboxylic acid) are believed to have the highest density of open metal sites.<sup>43</sup> In MOF-74, the dobdc<sup>4</sup> ligand (H<sub>4</sub>dobdc = 2,5-dihydroxyterephthalic acid) is fully deprotonated, leading to a simple stoichiometry of M<sub>2</sub>dobdc. From the formula alone, we could already deduce that the gravimetric density of metal sites in MOF-74 is exceptionally high (6.16 mmol/g for MOF-74-Zn, Table S1) and is in fact independent of crystal structure. The actual crystal structure affects the volumetric density (7.50 mmol/cm<sup>3</sup> for MOF-74-Zn) of metal sites. Of course, the percentage of metal sites that are available for guest binding (density of open metal sites) depends on crystal structure.

Towards the goal of creating MOFs with a high density of metal sites, we previously reported a charge-scaling model that led to the synthesis of CPM-47 (Li<sub>2</sub>obc, H<sub>2</sub>obc = 4-hydroxybenzoic acid) in which both gravimetric and volumetric density of solvent-binding metal sites exceed those of MOF-74 (13.3 mmol/g and 12.8 mmol/cm<sup>3</sup> for CPM-47). This strategy is based on the scale-down of charges on both metal ions (from 2+ to 1+) and ligands (from 4- to 2-) while maintaining the same metal-to-ligand (2:1) and phenolate-to-carboxylate ratios (1:1) as those in MOF-74.<sup>44</sup>

In this work, we propose a ligand charge-separation (LCS) model to target MOFs with a high metal-site density, using dobdc<sup>4</sup>- ligand as an illustrative example. An analysis of MOF-74 structures (M2dobdc) shows that by simply separating the phenolate and carboxylate functionality in H4dobdc into two separate chemical species, it is possible to create new crystal formulas capable of having the nearly same gravimetric density of metal sites. Such charge separation of H4dobdc ligand can be practically realized in different chemical compositions with various charge combinations (e.g., -3/-1 or -2/-1/-1). But the one that bears the closest resemblance to MOF-74 has the generic formula of M(II)2(OH)(obdc) with -3/-1 combination (H3obdc = 2-hydroxyterephthalic acid). Compared to MOF-74 type, the

<sup>&</sup>lt;sup>a</sup> Department of Chemistry and Biochemistry, California State University, Long Beach, California 90840, United States

<sup>&</sup>lt;sup>b</sup> Department of Chemistry, University of California, Riverside, California 92521, United States *Supporting Information Placeholder* 

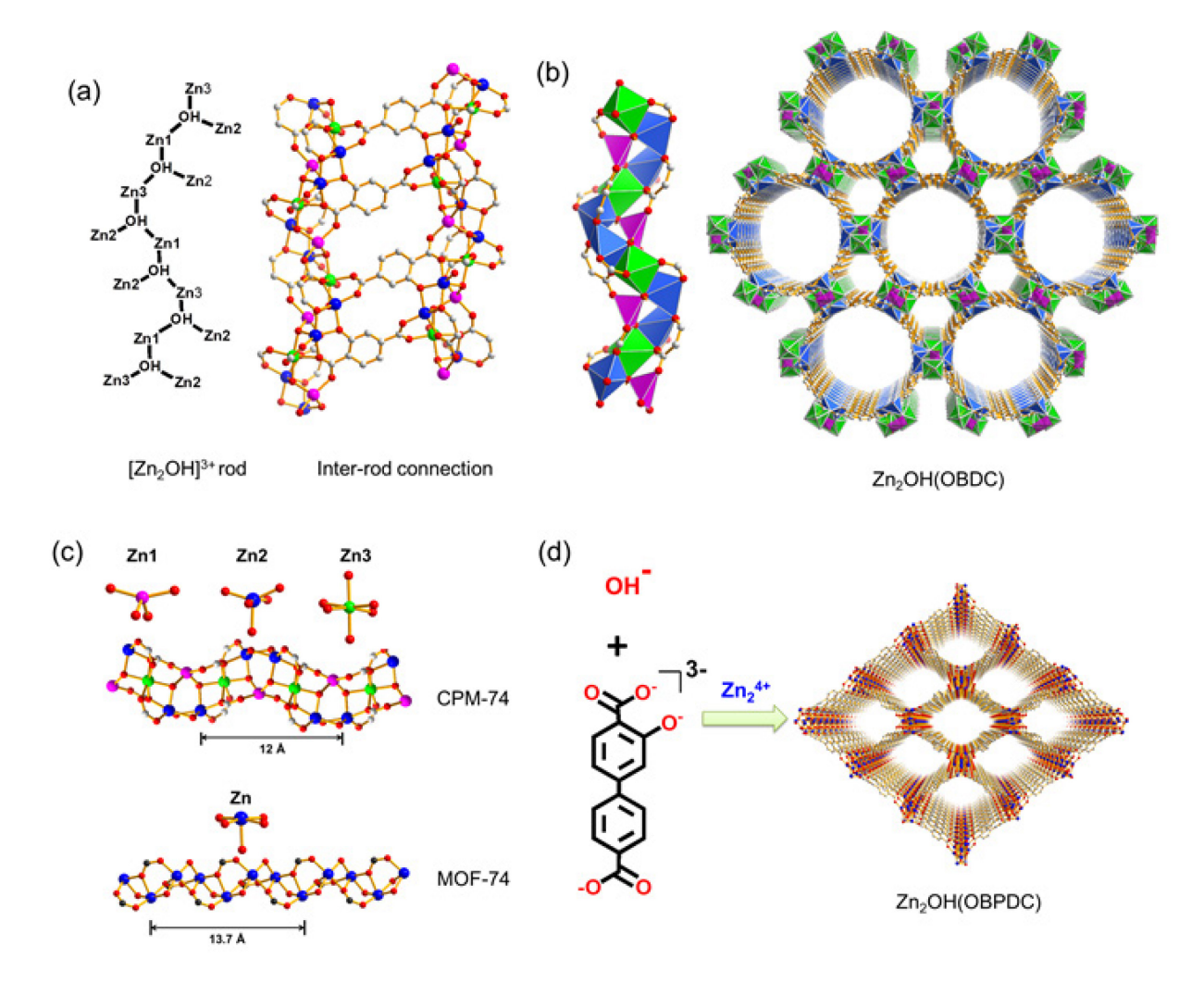


Figure 1. (a) ChemDraw representation of  $[Zn_2(OH)]^{3+}$  rod and ball-and-stick view of inter-rod connection. (b) Polyhedral view of the rod and the framework of **CPM-74**. (c) Comparison between the chains in CPM-74 and MOF-74. (d) Building Scheme of **CPM-75**. Zn1, pink; Zn2, blue; Zn3, green; C, gray; O, red.

hypothetical M(II)<sub>2</sub>(OH)(obdc) contains only two extra H-atoms and can be considered as quasi-isomers of MOF-74 (Scheme 1).

Theoretically, different crystal structures of generic M(II)<sub>2</sub>(OH)(obdc) or its elongated versions such as = 4-(4-carboxyphenyl)-2-M(II)<sub>2</sub>(OH)(obpdc) (H<sub>3</sub>obpdc hydroxybenzoic acid) are possible, and yet despite this simple stoichiometry and many structural possibilities, none has been known prior to this study. Here, we report two structure types (CPM-74 and CPM-75) that have been synthesized experimentally. Both structures are based on the packing of 1D [Zn<sub>2</sub>(OH)]<sup>3+</sup> rods which can be viewed as corner-sharing  $[Zn_3(OH)]^{5+}$  trimers. In **CPM-74**, all rods have the same handedness, leading to a chiral crystal structure. In CPM-75, rods of opposite handedness coexist, leading to an achiral crystal structure as is the case with MOF-74. Even though each individual crystal of CPM-74 is homochiral, the bulk sample is expected to be a racemic mixture with crystals of opposite

**CPM-74** has hexagonal symmetry with a chiral  $P6_122$  space group (cf. R-3 for MOF-74) and a framework formula of  $Zn_2(OH)(obdc)$  (Table S2). Its asymmetric unit contains three crystallographically unique Zn sites (Figure S3). While Zn2 is on the general position, both Zn1 and Zn3 are on the 2-fold rotation axes, giving the Zn1:Zn2:Zn3 ratio of 25:50:25. In the assynthesized form, Zn1 is 5-coordinate with two carboxylate

oxygens, two OH groups, and one pendent solvent. The Zn1-solvent bond is relatively strong at 2.10 Å and coincides with the 2-fold rotation axis. Zn2 is 6-coordinate with two carboxylate oxygens, two phenolate oxygens, one OH, and one pendent solvent. Because the coordination environment of Zn2 is more crowded than that of Zn1, the Zn2-solvent bond is relatively weak at 2.57 Å. Also, as suggested by high thermal parameters, these solvent sites around Zn2 are not fully occupied, even for assynthesized samples. Finally, Zn3, which accounts for 25% of total metal sites, has saturated coordination environment with two OH groups trans to each other and four carboxylate oxygens (Figure 1).

Excluding solvent coordination, the coordination numbers of Zn1, Zn2, and Zn3 are 4, 5, and 6, respectively with the average coordination number of 5, the same as that of desolvated MOF-74 in which all zinc sites have the same square-pyramidal coordination geometry. In the desolvated form of **CPM-74**, 25% of metal sites (Zn3) are saturated, however, another 25% of Zn sites (Zn1) are only 4-coordinate, leaving such metal sites wide open. The remaining zinc sites (Zn2, 50% of the total metal sites) have one guest binding site (Figure 1c). Open metal sites, while desirable for increasing host-guest affinity, can contribute to lower stability, both in terms of framework rigidity and the susceptibility to chemical attack. For this reason, it can be advantageous to have both saturated and unsaturated metal sites

with the former contributing to the framework stability and the latter serving as guest-binding sites. The ideal ratio between saturated and unsaturated metal sites would be dictated by the requirements of specific applications.

There is a clear resemblance between **CPM-74** and MOF-74 in both chemical composition and structural features. In fact, the equal ratio of obdc<sup>3-</sup> and OH<sup>-</sup> in **CPM-74** can be viewed as two subcomponents of dobdc<sup>4-</sup> in MOF-74. As such, **CPM-74** (formula: Zn<sub>2</sub>C<sub>8</sub>H<sub>4</sub>O<sub>6</sub>) has only two extra H-atoms than MOF-74 (formula: Zn<sub>2</sub>C<sub>8</sub>H<sub>2</sub>O<sub>6</sub>). The ArO<sup>-</sup>/ArCOO<sup>-</sup> side of obdc<sup>3-</sup> ligand in **CPM-74** also has the similar bonding mode to metal sites as that of MOF-74 (Figure S6). Besides, both structures are rare examples of MOFs with both phenolate and carboxylate groups. <sup>45,46</sup>

**CPM-74** features homo-helical rods linked together to give small trigonal and large hexagonal channels. The effective aperture of the hexagonal channel is 1.3 nm (Figure S5), slightly larger than that of MOF-74 (1.1 nm). The calculation by PLATON program gives the solvent-accessible volume of 49.5%, which lies between MOF-74Zn (58.2%) and its isomer UTSA-74 (47.8%).

CPM-75, Zn<sub>2</sub>(OH)(obpdc), was synthesized to demonstrate the general applicability of the proposed ligand charge separation model. Interestingly, while the charge separation model was confirmed again, a new structure type (CPM-75) with crystal symmetry of *Fddd* (Figure 1d) was obtained due to hetero-helical rod packing. Like CPM-74, CPM-75 also contains three crystallographically unique Zn sites in the ratio of 25:50:25 for Zn1:Zn2:Zn3 and nearly the same rod structure as CPM-74 (Figure S7), but its 3-D framework topology is different.

So far, the homo-helical form (denoted as CPM-74-II), which would be an isomer of CPM-75, but isoreticular to CPM-74, has not been synthesized. The formation of CPM-75 is likely caused by the difficulty to maintain coplanarity of two phenylene rings. It is possible that a ligand with three phenylene rings (similar to that in IRMOF-74-III) or other planar backbones may generate larger-pore structures (such as hypothetical CPM-74-III) that are isoreticular to CPM-74. Higher members of CPM-74 would be of particular interest because they would have parallel channels with different dimensions, a feature that is not found in IRMOF-74 series.

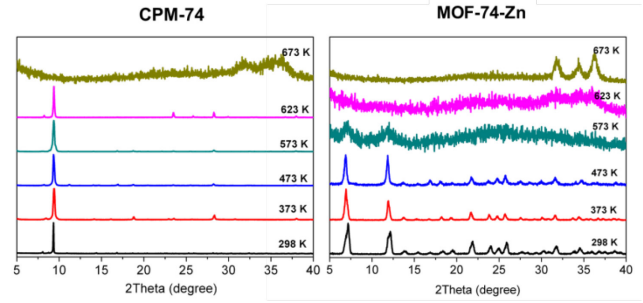
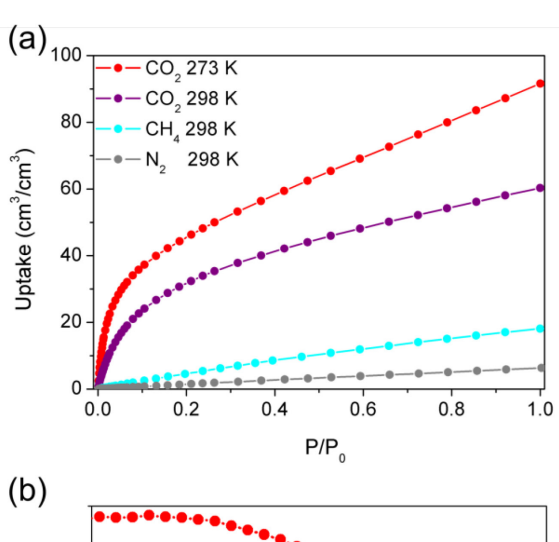


**Figure 2.** Comparison of thermal stability between **CPM-74** and MOF-74-Zn.

Thermal and hydrothermal stability of both CPM-74 and -75 is very high, especially when compared to other zinc MOFs. 47-50 ENREF 43 CPM-74 retains high crystallinity and is resistant to water upon exposure to aqueous solutions with pH ranging from 3 to 10 for at least 24 hours and the structure remained intact in boiling organic solvents and water (Figure S8). Temperature-dependent PXRD experiments show that CPM-74 can maintain the framework at 350 °C while MOF-74-Zn becomes noticeably less crystalline at 300 °C (Figure 2). The result was also supported by TGA analysis, demonstrating the

higher stability than that of MOF-74-Zn (Figure S9). One likely stabilizing factor is the 25% saturated Zn3 sites in CPM-74. In addition, CPM-75 was also found to exhibit high thermal and hydrothermal stability (Figure S10-11).

The gas adsorption properties of **CPM-74** and **-75** were investigated. The solvent-exchanged sample of **CPM-74** is activated at an optimized temperature of 300 °C. N<sub>2</sub> adsorption experiment at 77 K yielded a reversible type-I isotherm, demonstrating the permanent porosity (Figure S12). A BET surface area of 769 m²/g, and a Langmuir surface area of 1067 m²/g (cf. 1277 m²/g for MOF-74-Zn), with t-plot micropore volume of 0.37 cm³/g are determined. **CPM-74** is also found to have a moderate H<sub>2</sub> adsorption (1.3 wt%) at 77 K and 1atm (Figure S13). The BET surface area and Langmuir surface area for **CPM-75** are 1330 and 1515 m²/g (Figure S14), respectively and the uptake for H<sub>2</sub> is 1.7 wt% at 77 K and 1 atm (Figure S15).



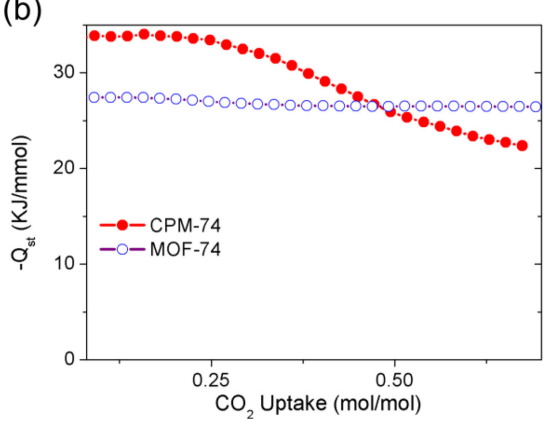


**Figure 3**. (a) Gas adsorption isotherms of **CPM-74**. (b) Comparisons of the CO<sub>2</sub> adsorption enthalpy between MOF-74 and **CPM-74**.

CPM-74 showed a high affinity towards CO<sub>2</sub>. The CO<sub>2</sub> uptake of CPM-74 at 273 K and even 298 K exhibited a steep increase at low pressure, indicating a high affinity. It has a saturation CO2 uptake of 91 cm<sup>3</sup>/cm<sup>3</sup> at 273 K. The isosteric heats of adsorption (Qst) near the zero coverage were calculated to be -33 kJ mmol<sup>-1</sup> and are significantly higher than MOF-74Zn (-27 kJ mmol<sup>-1</sup>) and UTSA-74 mmol<sup>-1</sup>) (-25)kJ at the low-pressure regime, 40,51 ENREF 16 and is comparable to those of MOF-74-Fe and MOF-74-Co (Figure 3). The stronger affinity of CPM-74 toward CO<sub>2</sub>, as compared to MOF-74-Zn, is also evident by comparing their low-pressure uptake. At 0.1 atm, MOF-74-Zn only takes around 1/4 of its saturation uptake, while CPM-74 takes up to 40% at the same condition. One probable factor for such a higher CO<sub>2</sub> affinity is the low coordination number of Zn1 (4, compared to 5 in MOF-74). The DFT calculations also show that Zn1 in **CPM-74** has a higher binding energy (31.3 kJ/mol) towards CO<sub>2</sub> than Zn site in MOF-74 (24.5 kJ/mol) (Figure S16). The selectivities for CO<sub>2</sub>/CH<sub>4</sub> and CO<sub>2</sub>/N<sub>2</sub> are calculated based on IAST theory. The results show that **CPM-74** has a high CO<sub>2</sub>/CH<sub>4</sub> (15-22 for CO<sub>2</sub>:CH<sub>4</sub> = 50:50) and CO<sub>2</sub>/N<sub>2</sub> (72-77 for CO<sub>2</sub>:N<sub>2</sub> = 10:90) selectivity at 298 K (Figure S17-20).

In conclusion, we introduce here a viable synthetic strategy to develop sets of ligand combinations (OH- and obdc3- or OH- and obpdc3- here) to create new structural types (CPM-74 and CPM-75 here) that functionally and stoichiometrically mimic parts of a higher all-in-one polyfunctional ligand (dobdc4- in this work) while conserving the total ligand charge (e.g. 3-/1- vs 4-). Materials created this way can be made to be quasi-isomeric with the established high-performance structure types (e.g., MOF-74), but have the potential for novel structural features and enhanced properties. This focused, yet broadly applicable approach targets specific chemical and structural features and is useful for developing new chemical systems. Moreover, this method can serve as a structure-analysis concept to help uncover structural and property correlations for seemingly unrelated materials (e.g., M<sub>2</sub>(dobdc) vs. M<sub>2</sub>(OH<sub>2</sub>)(bdc)).

## **ASSOCIATED CONTENT**

#### **Supporting Information**

The Supporting Information is available free of charge on the ACS Publications website.

Experimental Procedures and compound characterization data (PDF)

Crystallographic data for CPM-74 and CPM-75 (CIF)

#### **AUTHOR INFORMATION**

#### **Corresponding Author**

E-mail: \*xianhui.bu@csulb.edu; \*pingyun.feng@ucr.edu Notes

The authors declare no competing financial interests.

## **ACKNOWLEDGMENT**

We thank the support by NSF-DMR, under award NO. 1708850 (XB) and CSULB RSCA award (XB).

#### REFERENCE

- (1) Furukawa, H.; Cordova, K. E.; O'Keeffe, M.; Yaghi, O. M. The Chemistry and Applications of Metal-Organic Frameworks. *Science* **2013**, *341*, 1230444.
- (2) Farha, O. K.; Özgür Yazaydın, A.; Eryazici, I.; Malliakas, C. D.; Hauser, B. G.; Kanatzidis, M. G.; Nguyen, S. T.; Snurr, R. Q.; Hupp, J. T. De novo synthesis of a metal–organic framework material featuring ultrahigh surface area and gas storage capacities. *Nat. Chem.* **2010**, *2*, 944.
- (3) An, J.; Farha, O. K.; Hupp, J. T.; Pohl, E.; Yeh, J. I.; Rosi, N. L. Metal-adeninate vertices for the construction of an exceptionally porous metal-organic framework. *Nat. Comm.* **2012**, 3, 604.
- (4) Feng, D.; Liu, T.-F.; Su, J.; Bosch, M.; Wei, Z.; Wan, W.; Yuan, D.; Chen, Y.-P.; Wang, X.; Wang, K.; Lian, X.; Gu, Z.-Y.; Park, J.; Zou, X.; Zhou, H.-C. Stable metal-organic frameworks containing single-molecule traps for enzyme encapsulation. *Nat. Comm.* **2015**, *6*, 5979.

- (5) Furukawa, H.; Ko, N.; Go, Y. B.; Aratani, N.; Choi, S. B.; Choi, E.; Yazaydin, A. Ö.; Snurr, R. Q.; O'Keeffe, M.; Kim, J.; Yaghi, O. M. Ultrahigh Porosity in Metal-Organic Frameworks. *Science* **2010**, *329*, 424.
- (6) Deng, H.; Grunder, S.; Cordova, K. E.; Valente, C.; Furukawa, H.; Hmadeh, M.; Gándara, F.; Whalley, A. C.; Liu, Z.; Asahina, S.; Kazumori, H.; O'Keeffe, M.; Terasaki, O.; Stoddart, J. F.; Yaghi, O. M. Large-Pore Apertures in a Series of Metal-Organic Frameworks. *Science* **2012**, *336*, 1018.
- (7) Dolgopolova, E. A.; Rice, A. M.; Martin, C. R.; Shustova, N. B. Photochemistry and photophysics of MOFs: steps towards MOF-based sensing enhancements. *Chem. Soc. Rev.* **2018**, *47*, 4710
- (8) Schoedel, A.; Li, M.; Li, D.; O'Keeffe, M.; Yaghi, O. M. Structures of Metal-Organic Frameworks with Rod Secondary Building Units. *Chem. Rev.* **2016**, *116*, 12466.
- (9) Dincă, M.; Long, J. R. Hydrogen Storage in Microporous Metal-Organic Frameworks with Exposed Metal Sites. *Angew. Chem. Int. Ed.* **2008**, *47*, 6766.
- (10) Bloch, E. D.; Queen, W. L.; Krishna, R.; Zadrozny, J. M.; Brown, C. M.; Long, J. R. Hydrocarbon Separations in a Metal-Organic Framework with Open Iron(II) Coordination Sites. *Science* **2012**, *335*, 1606.
- (11) McDonald, T. M.; Lee, W. R.; Mason, J. A.; Wiers, B. M.; Hong, C. S.; Long, J. R. Capture of Carbon Dioxide from Air and Flue Gas in the Alkylamine-Appended Metal-Organic Framework mmen-Mg<sub>2</sub>(dobpdc). *J. Am. Chem. Soc.* **2012**, *134*, 7056.
- (12) Zhou, W.; Wu, H.; Yildirim, T. Enhanced H<sub>2</sub> Adsorption in Isostructural Metal-Organic Frameworks with Open Metal Sites: Strong Dependence of the Binding Strength on Metal Ions. *J. Am. Chem. Soc.* **2008**, *130*, 15268.
- (13) Cozzolino, A. F.; Brozek, C. K.; Palmer, R. D.; Yano, J.; Li, M.; Dincă, M. Ligand Redox Non-innocence in the Stoichiometric Oxidation of Mn<sub>2</sub>(2,5-dioxidoterephthalate) (Mn-MOF-74). *J. Am. Chem. Soc.* **2014**, *136*, 3334.
- (14) Feng, L.; Li, J.-L.; Day, G. S.; Lv, X.-L.; Zhou, H.-C. Temperature-Controlled Evolution of Nanoporous MOF Crystallites into Hierarchically Porous Superstructures. *Chem* **2019**, *5*, 1265.
- (15) Cai, G.; Zhang, W.; Jiao, L.; Yu, S.-H.; Jiang, H.-L. Template-Directed Growth of Well-Aligned MOF Arrays and Derived Self-Supporting Electrodes for Water Splitting. *Chem* **2017**, *2*, 791.
- (16) Pachfule, P.; Shinde, D.; Majumder, M.; Xu, Q. Fabrication of carbon nanorods and graphene nanoribbons from a metalorganic framework. *Nat. Chem.* **2016**, *8*, 718.
- (17) Li, S.-L.; Xu, Q. Metal–organic frameworks as platforms for clean energy. *Energy & Environmental Science* **2013**, *6*, 1656.
- (18) Pan, M.; Liao, W.-M.; Yin, S.-Y.; Sun, S.-S.; Su, C.-Y. Single-Phase White-Light-Emitting and Photoluminescent Color-Tuning Coordination Assemblies. *Chem. Rev.* **2018**, *118*, 8889.
- (19) Xu, C.; Fang, R.; Luque, R.; Chen, L.; Li, Y. Functional metal—organic frameworks for catalytic applications. *Coord. Chem. Rev.* **2019**, *388*, 268.
- (20) Zhao, X.; Wang, Y.; Li, D.-S.; Bu, X.; Feng, P. Metal-Organic Frameworks for Separation. *Adv. Mater.* **2018**, *30*, 1705189.
- (21) Nugent, P.; Belmabkhout, Y.; Burd, S. D.; Cairns, A. J.; Luebke, R.; Forrest, K.; Pham, T.; Ma, S.; Space, B.; Wojtas, L.; Eddaoudi, M.; Zaworotko, M. J. Porous materials with optimal adsorption thermodynamics and kinetics for CO<sub>2</sub> separation. *Nature* **2013**, *495*, 80.
- (22) Cui, X.; Chen, K.; Xing, H.; Yang, Q.; Krishna, R.; Bao, Z.; Wu, H.; Zhou, W.; Dong, X.; Han, Y.; Li, B.; Ren, Q.; Zaworotko, M. J.; Chen, B. Pore chemistry and size control in

- hybrid porous materials for acetylene capture from ethylene. *Science* **2016**, *353*, 141.
- (23) Cadiau, A.; Adil, K.; Bhatt, P. M.; Belmabkhout, Y.; Eddaoudi, M. A metal-organic framework-based splitter for separating propylene from propane. *Science* **2016**, *353*, 137.
- (24) Caskey, S. R.; Wong-Foy, A. G.; Matzger, A. J. Dramatic Tuning of Carbon Dioxide Uptake via Metal Substitution in a Coordination Polymer with Cylindrical Pores. *J. Am. Chem. Soc.* **2008**, *130*, 10870.
- (25) Xiang, S.; Zhou, W.; Zhang, Z.; Green, M. A.; Liu, Y.; Chen, B. Open Metal Sites within Isostructural Metal—Organic Frameworks for Differential Recognition of Acetylene and Extraordinarily High Acetylene Storage Capacity at Room Temperature. *Angew. Chem. Int. Ed.* **2010**, *49*, 4615.
- (26) Liao, P.-Q.; Chen, H.; Zhou, D.-D.; Liu, S.-Y.; He, C.-T.; Rui, Z.; Ji, H.; Zhang, J.-P.; Chen, X.-M. Monodentate hydroxide as a super strong yet reversible active site for CO<sub>2</sub> capture from high-humidity flue gas. *Energy Environ. Sci.* **2015**, *8*, 1011.
- (27) Lu, X.-F.; Liao, P.-Q.; Wang, J.-W.; Wu, J.-X.; Chen, X.-W.; He, C.-T.; Zhang, J.-P.; Li, G.-R.; Chen, X.-M. An Alkaline-Stable, Metal Hydroxide Mimicking Metal-Organic Framework for Efficient Electrocatalytic Oxygen Evolution. *J. Am. Chem. Soc.* 2016, *138*, 8336.
- (28) FitzGerald, S. A.; Pierce, C. J.; Rowsell, J. L. C.; Bloch, E. D.; Mason, J. A. Highly Selective Quantum Sieving of D<sub>2</sub> from H<sub>2</sub> by a Metal-Organic Framework As Determined by Gas Manometry and Infrared Spectroscopy. *J. Am. Chem. Soc.* **2013**, *135*, 9458.
- (29) Thallapally, P. K.; Grate, J. W.; Motkuri, R. K. Facile xenon capture and release at room temperature using a metal-organic framework: a comparison with activated charcoal. *Chem. Commun.* **2012**, *48*, 347.
- (30) Morris, R. E.; Brammer, L. Coordination change, lability and hemilability in metal–organic frameworks. *Chem. Soc. Rev.* **2017**, *46*, 5444.
- (31) Henkelis, S. E.; McCormick, L. J.; Cordes, D. B.; Slawin, A. M.; Morris, R. E. Synthesis and crystallographic characterisation of Mg(H<sub>2</sub>dhtp)(H<sub>2</sub>O)<sub>5</sub>· H<sub>2</sub>O. *Inorg. Chem. Commun.* **2016**, *65*, 21. (32) Li, B.; Chrzanowski, M.; Zhang, Y.; Ma, S. Applications of metal-organic frameworks featuring multi-functional sites. *Coord. Chem. Rev.* **2016**, *307*, 106.
- (33) Li, B.; Leng, K.; Zhang, Y.; Dynes, J. J.; Wang, J.; Hu, Y.; Ma, D.; Shi, Z.; Zhu, L.; Zhang, D.; Sun, Y.; Chrzanowski, M.; Ma, S. Metal-Organic Framework Based upon the Synergy of a Brønsted Acid Framework and Lewis Acid Centers as a Highly Efficient Heterogeneous Catalyst for Fixed-Bed Reactions. *J. Am. Chem. Soc.* 2015, *137*, 4243.
- (34) Li, H.; Shi, W.; Zhao, K.; Niu, Z.; Li, H.; Cheng, P. Highly Selective Sorption and Luminescent Sensing of Small Molecules Demonstrated in a Multifunctional Lanthanide Microporous Metal–Organic Framework Containing 1D Honeycomb-Type Channels. *Chem. Eur. J.* **2013**, *19*, 3358.
- (35) Rosi, N. L.; Kim, J.; Eddaoudi, M.; Chen, B.; O'Keeffe, M.; Yaghi, O. M. Rod Packings and Metal—Organic Frameworks Constructed from Rod-Shaped Secondary Building Units. *J. Am. Chem. Soc.* **2005**, *127*, 1504.
- (36) Dietzel, P. D. C.; Panella, B.; Hirscher, M.; Blom, R.; Fjellvåg, H. Hydrogen adsorption in a nickel based coordination polymer with open metal sites in the cylindrical cavities of the desolvated framework. *Chem. Commun.* **2006**, *9*, 959.
- (37) Dietzel, P. D. C.; Morita, Y.; Blom, R.; Fjellvåg, H. An In Situ High-Temperature Single-Crystal Investigation of a Dehydrated Metal-Organic Framework Compound and Field-Induced Magnetization of One-Dimensional Metal-Oxygen Chains. *Angew. Chem. Int. Ed.* **2005**, *44*, 6354.
- (38) Kapelewski, M. T.; Geier, S. J.; Hudson, M. R.; Stück, D.; Mason, J. A.; Nelson, J. N.; Xiao, D. J.; Hulvey, Z.; Gilmour, E.;

- FitzGerald, S. A.; Head-Gordon, M.; Brown, C. M.; Long, J. R. M2(m-dobde) (M = Mg, Mn, Fe, Co, Ni) Metal-Organic Frameworks Exhibiting Increased Charge Density and Enhanced H2 Binding at the Open Metal Sites. *J. Am. Chem. Soc.* **2014**, *136*, 12119.
- (39) Kapelewski, M. T.; Runčevski, T.; Tarver, J. D.; Jiang, H. Z. H.; Hurst, K. E.; Parilla, P. A.; Ayala, A.; Gennett, T.; FitzGerald, S. A.; Brown, C. M.; Long, J. R. Record High Hydrogen Storage Capacity in the Metal–Organic Framework Ni2(m-dobdc) at Near-Ambient Temperatures. *Chem. Mater.* **2018**, *30*, 8179.
- (40) Luo, F.; Yan, C.; Dang, L.; Krishna, R.; Zhou, W.; Wu, H.; Dong, X.; Han, Y.; Hu, T.-L.; O'Keeffe, M.; Wang, L.; Luo, M.; Lin, R.-B.; Chen, B. UTSA-74: A MOF-74 Isomer with Two Accessible Binding Sites per Metal Center for Highly Selective Gas Separation. *J. Am. Chem. Soc.* **2016**, *138*, 5678.
- (41) Sun, L.; Miyakai, T.; Seki, S.; Dincă, M. Mn<sub>2</sub>(2,5-disulfhydrylbenzene-1,4-dicarboxylate): A Microporous Metal–Organic Framework with Infinite (−Mn−S−)∞ Chains and High Intrinsic Charge Mobility. *J. Am. Chem. Soc.* **2013**, *135*, 8185.
- (42) Sun, L.; Hendon, C. H.; Minier, M. A.; Walsh, A.; Dincă, M. Million-Fold Electrical Conductivity Enhancement in Fe<sub>2</sub>(DEBDC) versus Mn<sub>2</sub>(DEBDC) (E = S, O). *J. Am. Chem. Soc.* **2015**, *137*, 6164.
- (43) Liang, L.; Liu, C.; Jiang, F.; Chen, Q.; Zhang, L.; Xue, H.; Jiang, H.-L.; Qian, J.; Yuan, D.; Hong, M. Carbon dioxide capture and conversion by an acid-base resistant metal-organic framework. *Nat. Comm.* **2017**, *8*, 1233.
- (44) Zhao, X.; Shimazu, M. S.; Chen, X.; Bu, X.; Feng, P. Homo-Helical Rod Packing as a Path Toward the Highest Density of Guest-Binding Metal Sites in Metal-Organic Frameworks. *Angew. Chem. Int. Ed.* **2018**, *57*, 6208.
- (45) Hong, K.; Bak, W.; Chun, H. Unique Coordination-Based Heterometallic Approach for the Stoichiometric Inclusion of High-Valent Metal Ions in a Porous Metal-Organic Framework. *Inorg. Chem.* **2013**, *52*, 5645.
- (46) Wu, D.; Yan, W.; Xu, H.; Zhang, E.; Li, Q. Defect engineering of Mn-based MOFs with rod-shaped building units by organic linker fragmentation. *Inorg. Chim. Acta* **2017**, *460*, 93.
- (47) Kaye, S. S.; Dailly, A.; Yaghi, O. M.; Long, J. R. Impact of Preparation and Handling on the Hydrogen Storage Properties of Zn4O(1,4-benzenedicarboxylate)3 (MOF-5). *J. Am. Chem. Soc.* **2007**, *129*, 14176.
- (48) Ding, N.; Li, H.; Feng, X.; Wang, Q.; Wang, S.; Ma, L.; Zhou, J.; Wang, B. Partitioning MOF-5 into Confined and Hydrophobic Compartments for Carbon Capture under Humid Conditions. *J. Am. Chem. Soc.* **2016**, *138*, 10100.
- (49) Liu, L.; Konstas, K.; Hill, M. R.; Telfer, S. G. Programmed Pore Architectures in Modular Quaternary Metal—Organic Frameworks. *J. Am. Chem. Soc.* **2013**, *135*, 17731.
- (50) Koh, K.; Wong-Foy, A. G.; Matzger, A. J. A Porous Coordination Copolymer with over 5000 m<sup>2</sup>/g BET Surface Area. *J. Am. Chem. Soc.* **2009**, *131*, 4184.
- (51) Queen, W. L.; Hudson, M. R.; Bloch, E. D.; Mason, J. A.; Gonzalez, M. I.; Lee, J. S.; Gygi, D.; Howe, J. D.; Lee, K.; Darwish, T. A.; James, M.; Peterson, V. K.; Teat, S. J.; Smit, B.; Neaton, J. B.; Long, J. R.; Brown, C. M. Comprehensive study of carbon dioxide adsorption in the metal—organic frameworks M2(dobdc) (M = Mg, Mn, Fe, Co, Ni, Cu, Zn). *Chemical Science* **2014**, *5*, 4569.

# TOC

